Supplementary Material

1 SUPPLEMENTARY DATA

1.1 Petrography

Polarized light microscope petrography is used to help identify the non-indexed phase (Fig. S1). The petrography shows that the samples are composed of quartz, plagioclase, garnet and sheet-like mica between these minerals.

1.2 EWAVE Sensitivity to Fracture Shape and Size

Two parameters associated with porosity are tested. The sample used for this testing is a protomylonite collected from Stony Creek (further referred to as the test sample) of which the EBSD data and lab P-wave velocity measurement are published in Adam et al. (2020). Similar to sample used in this study, phyllosilicate minerals in the test sample couldn't be index and mica was assumed to align perfectly with the foliation. The first parameter is the fracture shape. To do this, two fracture shapes of roughly the same size are used: (a) 2 px by 10 px fracture (5:1 aspect ratio; 20 px squared area), and (b) 4 px by 4 px fracture (1:1 aspect ratio; 16 px squared area). The second parameter is the fracture size. For this, model (a) is compared to model (c): a 4-px-by-20-px fracture (5:1 aspect ratio; same as model (a) (Fig. S2). The fracture dimension for the test sample are shown in Figure S3. By adding fractures with a volume equal to 2% porosity, the velocity decreases in both the fast and the slow directions. For the 4 px by 4 px pore, the fast and slow velocities decrease by a similar amount thus, resulting in this fractured rock having similar elastic wave anisotropy to the pore-free rock. For the two flat shape fractures, the fast velocity decreases less than the slow velocity which then enhances the elastic wave anisotropy. The two flat shape pores produce almost identical modeled velocities regardless of the pore size.

1.3 Mica Orientation testing

In this study, mica orientation cannot be indexed via EBSD experiments. According to the petrographic images (Fig. S1), most mica align with the foliation. To determine the mica orientation, the test sample EBSD data and P-wave velocity measurement under elevated effective pressure are used. We fill the non-index phase of the test sample with mica which aligns with the foliation and randomly oriented mica at different volume fraction for a total of 6 models. Hills average (via MTEX Toolbox) is then used to calculate the fast and slow P-wave velocity of all 6 models. The velocities are compared to the lab velocity measurement under the highest available (64 MPa) effective pressure (Fig. S4). The lab and model data intersect where between 80% to 90% of mica align with the foliation. We extrapolated that the mica in this study align similarly. Therefore, a mica model with 80% aligned mica and 20% random mica is used to fill the non-index phase of the EBSD data in this study.

1.4 Additional GassDEM P-wave Velocity Results

Velocities and anisotropy of the sections cut 30^o to foliation with 5:1 aspect ratio fractures are also modeled (Fig. S5). The models yield higher slow P-wave speeds and lower anisotropy compared to those of the 90^o sections. The fast and slow velocities decrease from 6.5 km/s and 6.0 km/s (0% porosity) to 6.4 km/s and 5.1 km/s (5% porosity), respectively. The pore-free anisotropy of these samples ranges from 5-10% and increases to 20% when a 5 % of fractures are added. The slow velocity differences in the two sections stem from wave propagation direction during the slow velocity modeling. For the 90^o section, the Ricker wave is propagated perpendicular to foliation. For the 30^o section however, the wave is propagated 30^o to foliation. Because of this, the slow velocities from the 30^o section modeling are higher than the 90^o

section slow velocities and anisotropy lower. To accurately model the slow velocity and anisotropy, the 90^o section should be used. The modeled velocities and anisotropy of the pore-free 90^o and 30^o sections using GassDEM model are almost identical because of their similar mineral composition. In addition, P-wave velocities and anisotropy of the water-filled samples are also modeled (Fig. S6). The results are almost identical to those of air-filled fractures.

2 SUPPLEMENTARY TABLES AND FIGURES

2.1 Figures

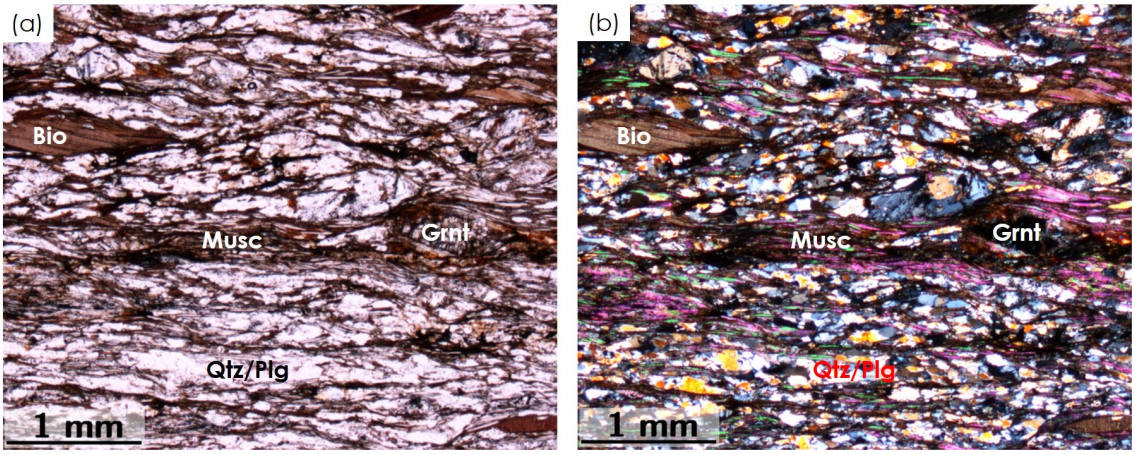

Figure S1. (a) Plane polarized, and (b) cross polarized microphotograph of the schist sample cut perpendicular to foliation. Bio = biotite, Musc = muscovite. Grnt = garnet, Qtz = quartz, Plg = plagioclase.

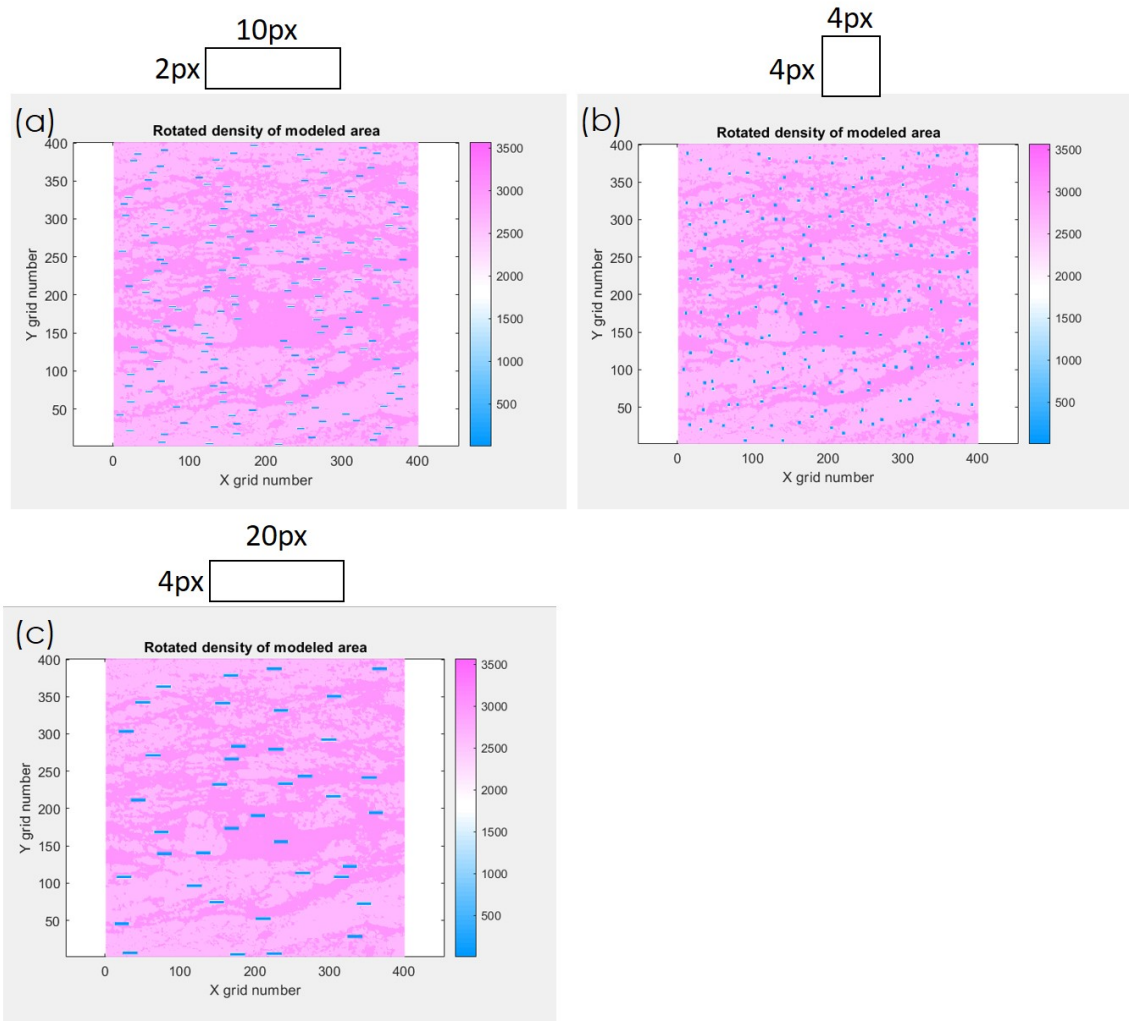

Figure S2. Models to test the effect of pore shape and size on effective elastic wave speeds. The total porosity for each of these three models is constant at 2%. The pore shapes are (a) 2 px by 10 px, (b) 4 px by 4 px, and (c) 4 px by 20 px. Pore shape is studied by comparing (a) to (b), while pore size is studied by comparing (a) to (c). The color scale represents the component phase density with blue being air-filled pores.

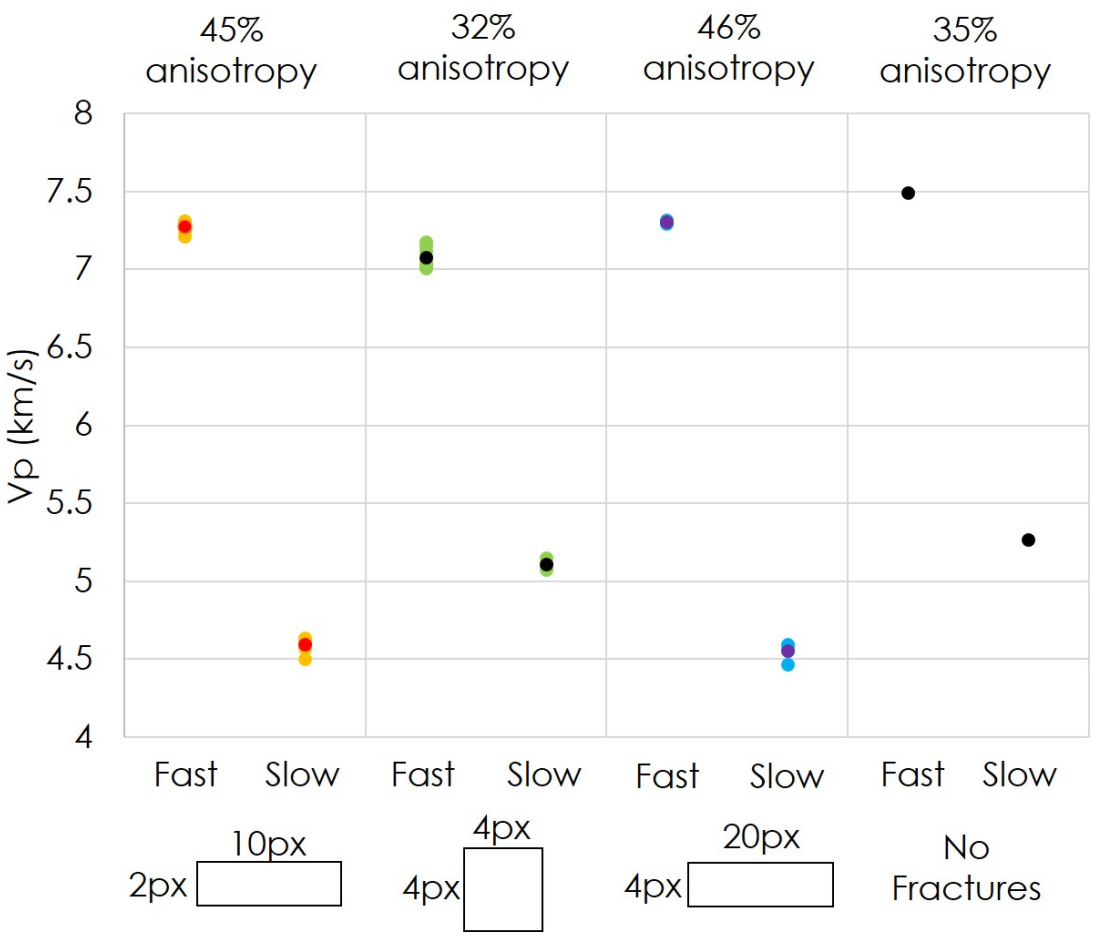

Figure S3. EWAVE modeled fast, slow P-wave velocities and anisotropy for 2% porosity test sample. Different pore shapes and distributions are compared. The modeled velocities of the pore-free sample are presented for reference. The light-colored data points are the modeled velocities using different randomly distributed pore models generated with the same pore shape and porosity. The dark-colored data points are the arithmetic mean of all pore distribution for the same pore shape.

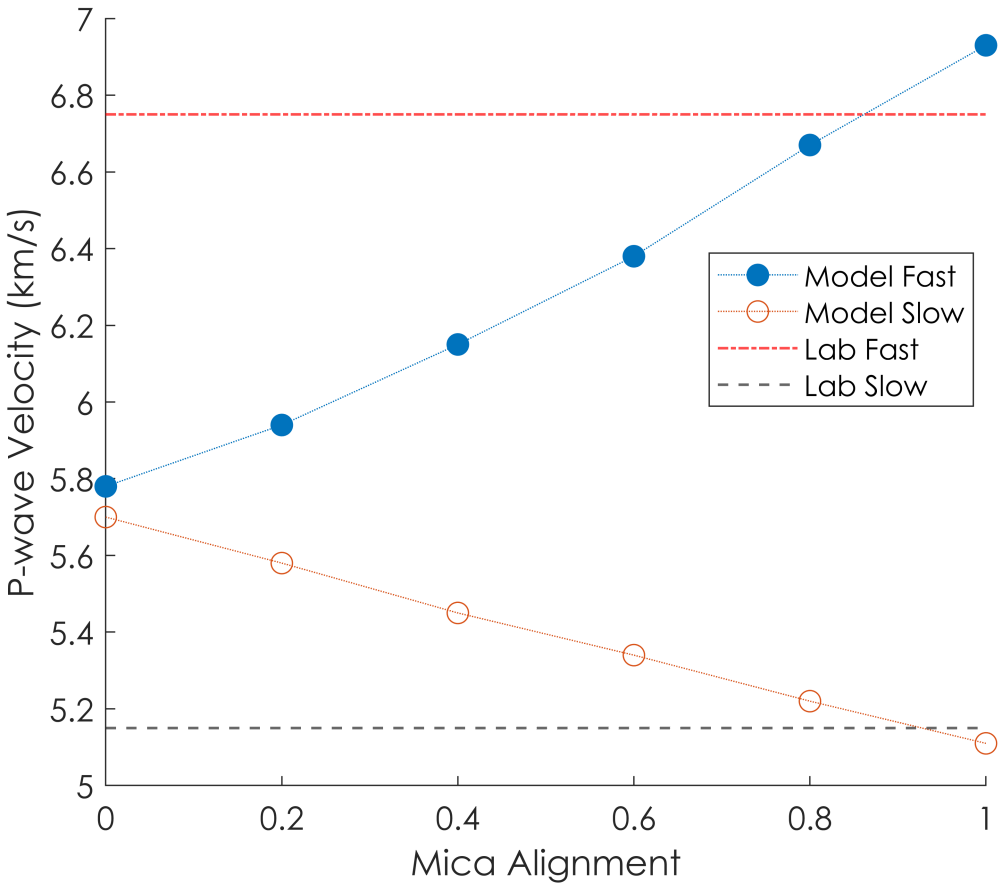

Figure S4. Modeled fast (blue) and slow (orange) P-wave velocities calculated using Hill average based on test samples with varying mica alignment models. The X-axis denotes mica alignment ranges from 0 (randomly oriented mica) to 1 (perfectly aligned mica). The red and black horizontal lines are fast and slow velocities from lab measurement presented in Adam et al. (2020) under 64 MPa effective pressure.

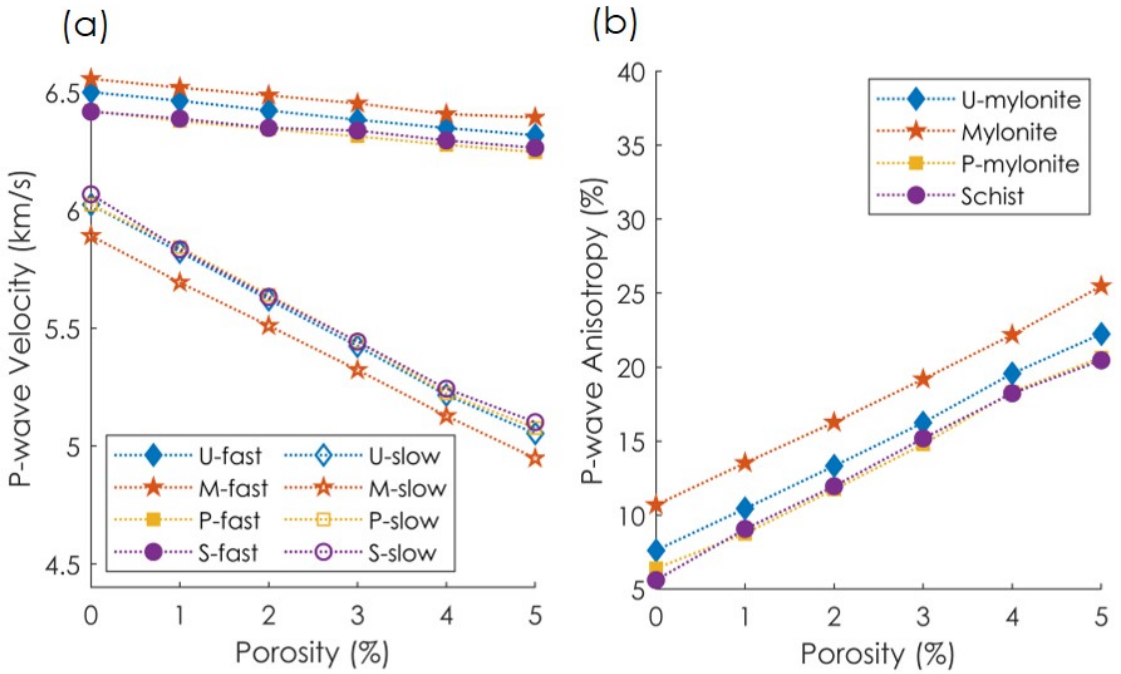

Figure S5. EWAVE modeling (5:1 fracture aspect ratio) of (a) P-wave velocities and (b) anisotropy of the samples cut 30^o to foliation.

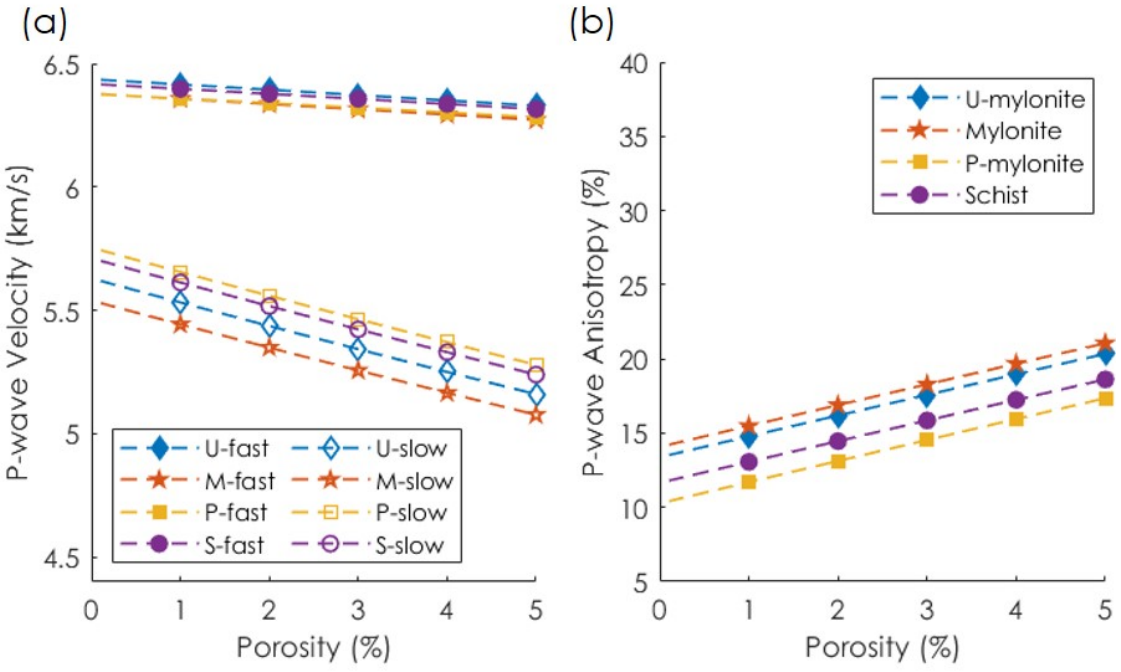

Figure S6. (a) P-wave velocities and (b) anisotropy model results of the water-filled samples modeled with GassDEM code.

2.2 Tables

Table S1. Fast and slow P-wave velocity (in km/s), and anisotropy results from EWAVE modeling.

	Pore-free			5% Porosity		
	Fast	Slow	Anisotropy	Fast	Slow	Anisotropy
Ultramylonite	6.41	5.83	9.47	6.26	4.67	29.24
Mylonite	6.48	5.55	15.50	6.35	4.47	34.79
Protomylonite	6.45	5.84	6.92	6.35	4.66	30.73
Schist	6.48	5.71	12.58	6.35	4.59	32.27

Table S2. Fast and slow P-wave velocity (in km/s), and anisotropy results from GassDEM modeling.

	0.1% Porosity			5% Porosity		
	Fast	Slow	Anisotropy	Fast	Slow	Anisotropy
Ultramylonite	6.44	5.62	13.54	6.38	5.15	21.27
Mylonite	6.38	5.53	14.23	6.32	5.07	22.02
Protomylonite	6.39	5.76	10.43	6.35	5.30	18.20
Schist	6.42	5.70	11.82	6.37	5.24	19.50

Table S3. Fast and slow P-wave velocity (in km/s), and anisotropy results from EWAVE and GassDEM modeling with 5:1 (2D), 5:2:1 (3D), and 5:5:1 (3D) fracture aspect ratio. The pore-free velocity results of the GassDEM model refer to the results using 0.1% fracture porosity.

	Pore-free			5% Porosity		
	Fast	Slow	Anisotropy	Fast	Slow	Anisotropy
EWAVE 5:1	6.45	5.84	9.92	6.35	4.66	30.73
GassDEM 5:2:1	6.34	5.75	10.43	6.35	5.29	18.20
GassDEM 5:5:1	6.34	5.75	10.58	6.33	4.92	25.15